Soil Surface Roughness Characteristics Under Different Agricultural Tillage Practices—A Case Study in the Black Soil Region of Northeast China

Zhuangzhuang Feng, Xingming Zheng, *Member, IEEE*, Xiaofeng Li, *Member, IEEE*, Huanjun Liu, Zui Tao, Chunmei Wang, Linghua Meng, Tianhao Guo, Jia Zheng, and Jinfeng Song

***Abstract*—Soil surface roughness (SSR) is an important factor affecting soil erosion and soil nutrient transport. Human tillage leads to increased instability in SSR, and the characteristics of SSR caused by different tillage practices await further study. This research utilizes terrestrial laser scanning (TLS) to measure the SSR of six farmland plots (25 m × 25 m) and analyzes the characteristics of SSR under different tillage practices (plowing, harrowing, ridging, crusting, etc.). The study results show: 1) Different agricultural tillage practices lead to significant differences in SSR. The plowed and harrowed plot corresponds to the maximum (2.49 cm) and minimum (1.5 cm) root mean square height (RMSH), respectively. Correlation length (CL) is more affected by different tillage practices than RMSH. The difference in CL between the ridged and harrowed plot is 2.6 times. 2) Ridging and crusting caused significant directional variation in SSR. The SSR anisotropy of the harrowed plot can be disregarded. 3) Under the condition of measuring soil profile in 12 directions and randomly sampling 70 times in each direction, the profile length must be at least 3 m to ensure that the measurement error of SSR is better than 5% compared to the "true" value. TLS can measure two-dimensional SSR. Therefore, it is only necessary to ensure that the measurement range is at least 3 m × 3 m. The study results provide a reference for the high-precision measurement of SSR (RMSH and CL) under different agricultural tillage practices.**

Manuscript received 28 February 2024; revised 13 May 2024; accepted 21 May 2024. Date of publication 28 May 2024; date of current version 14 June 2024. This work was supported in part by the National Key Research and Development Project of China under Grant 2021YFD1500103, in part by Strategic Priority Research Program of the Chinese Academy of Sciences under Grant XDA28100500, in part by the National Natural Science Foundation of China under Grant 42371381 and Grant 42201435, in part by Science and Technology Development Plan Project of Jilin Province under Grant 20210201044GX, and in part by Land Observation Satellite Supporting Platform of National Civil Space Infrastructure Project under Grant CASPLOS-CCSI. *(Corresponding author: Xingming Zheng.)*

Zhuangzhuang Feng, Tianhao Guo, Jia Zheng, and Jinfeng Song are with the State Key Laboratory of Black Soils Conservation and Utilization, Northeast Institute of Geography and Agroecology, Chinese Academy of Sciences, Changchun 130102, China, and also with the University of Chinese Academy of Sciences, Beijing 100049, China (e-mail: fengzhuangzhuang@iga.ac.cn; guotianhao@iga.ac.cn; zhengjia@iga.ac.cn; songjinfeng23@mails.ucas.ac.cn).

Xingming Zheng, Xiaofeng Li, Huanjun Liu, and Linghua Meng are with the State Key Laboratory of Black Soils Conservation and Utilization, Northeast Institute of Geography and Agroecology, Chinese Academy of Sciences, Changchun 130102, China (e-mail: zhengxingming@iga.ac.cn; lixiaofeng@iga.ac.cn; liuhuanjun@iga.ac.cn; menglinghua@iga.ac.cn).

Zui Tao and Chunmei Wang are with the Aerospace Information Research Institute, Chinese Academy of Sciences, Beijing 100094, China (e-mail: taozui@aircas.ac.cn; wangcm@aircas.ac.cn).

Digital Object Identifier 10.1109/JSTARS.2024.3405952

***Index Terms*—Agriculture, black soil region, soil surface roughness (SSR), terrestrial laser scanning (TLS), tillage practices.**

I. Introduction

SOIL surface roughness (SSR) is a topic of interest to various disciplines concerned with natural processes. As a basic physical property of soil, SSR is an important influencing factor for soil erosion, soil moisture distribution, and soil nutrient transport [1], [2]. Greater roughness increases the exposure of the soil surface, accelerating the erosion process of water flow and wind on the soil [3]. In addition, SSR is a key parameter in the microwave remote sensing inversion of soil moisture [4]. In some cases, its impact on the microwave signal may be greater than that of soil moisture [5]. Accurate monitoring of SSR is of great significance for the establishment of soil erosion process models, hydrological process simulation, and microwave remote sensing inversion of soil moisture [6].

SSR is usually measured by the root mean square height (RMSH) and correlation length (CL) in vertical and horizontal directions [7]. In addition, the autocorrelation function (ACF) is also an important parameter for describing SSR, including exponential and Gaussian functions. Agricultural soils are typically assumed to follow an exponential function [8].

The field measurement of SSR has evolved from one-dimensional profile measurement (pin profiler, board profiler, one-dimensional laser profiler) to two-dimensional surface measurement [photogrammetry, light detection and ranging (LiDAR), etc.] [9], [10], [11]. The two-dimensional methods for parameterizing SSR are much more accurate than traditional one-dimensional profile methods. They can accurately characterize the surface while meeting the basic assumptions of stationarity required by most backscatter models, which one-dimensional profile methods usually cannot achieve [12], [13]. LiDAR technology uses laser scanners and distance sensors to obtain the surface morphology of the target. Depending on the sensor payload platform, it is divided into spaceborne LiDAR, airborne LiDAR, and terrestrial laser scanning (TLS), etc. [14]. Spaceborne and airborne LiDAR, due to the coarse resolution of the laser spot, struggle to meet the measurement needs of field roughness at the centimeter scale. TLS, with its high point cloud density, fast speed, and millimeter-level ranging accuracy, can

extract and analyze the periodic and random characteristics of SSR, providing the possibility for scale decomposition of SSR information [15].

The feasibility and accuracy of contact SSR measurement methods (pin profilers and roller chains, etc.) and noncontact SSR measurement techniques (one-dimensional laser profilers, TLS, stereophotogrammetry, Xtion Pro method, etc.) have been evaluated previously [10], [15], [16], [17], [18], [19]. The results show that TLS not only ensures the highest accuracy and resolution in outdoor environments but also creates representative three-dimensional images containing more information.

In addition, the estimation of SSR by laser scanners has been evaluated on different payload platforms such as ground-based, airborne, etc. [14], [20], [21], [22], [23]. Turner et al. [14] proved that the RMSH estimated by airborne LiDAR is accurate enough to track the temporal variation of SSR in the vertical direction. However, CL estimates derived from airborne LiDAR cannot serve as an effective substitute for field measurements of CL. It was confirmed in [23] that pin profilers could be replaced by TLS for the accurate characterization of SSR.

The measurement and preprocessing methods of SSR have been quantitatively analyzed, including factors such as sampling interval, sampling profile length, number of repeat samplings, directionality of one-dimensional profile sampling, point cloud measurement density, and point cloud data interpolation methods [7], [24], [25], [26], [27]. For example, the study by Zheng et al. [27] concluded that under the conditions of more than 20 repeat samplings, a sampling interval of less than 10 mm, and a profile length of 200 times the CL, the measurement accuracy of field SSR is about 80%. Similarly, according to Bryant et al. [28], considering the heterogeneity of natural surfaces, at least 20 three-meter-long profile length should be collected to obtain a representative RMSH measurement.

However, SSR is both dominated by tillage (plowing tools and tillage practices) and constrained by soil aggregate structure and various external natural forces (rainfall, wind erosion, gravitational settling) [29]. Under modern agricultural production practices, tillage often leads to increased instability in SSR. The diversity of traditional tillage, conservative tillage, and organic tillage practices also poses new challenges in understanding the characteristics of field SSR. In some traditional agricultural areas, traditional tillage practices such as plowing, harrowing, and ridging are still commonly used [20]. In addition, conservation tillage practices such as no-till and reduced-till, which aim to reduce soil disturbance, are also advocated [30]. The application of any tillage practice is directly related to the improvement of soil physical properties (soil structure and SSR), and in turn, affects crop growth and yield.

The impact of agricultural tillage practices on the foreign farmland SSR has been studied. For example, Thomsen et al. [15] used TLS to measure the SSR of 1 m^2 agricultural plots in southern Norway under different tillage practices (plowing, harrowing, forest, and direct seeding on stubble). Davenport et al. [20] used airborne LiDAR data to identify the RMSH of different tillage plots without quantitative comparison with ground measurements. It is worth noting that the farmland SSR under different tillage practices has scale differences and regional differences. SSR measured in small areas locally usually cannot well represent the surrounding environment [14]. Furthermore, due to differences in geographical locations and climatic conditions, agricultural tillage practices vary significantly among different countries, leading to substantial differences in SSR. There is limited research on the SSR under different tillage practices in the black soil region of Northeast China. We aim to examine the effects of different tillage practices, including plowing, harrowing, ridging, and crusting, on the SSR characteristics of representative large farmland plots (25 m $\times$ 25 m). This study seeks to enhance the accuracy of erosion and microwave remote sensing soil moisture models, as well as deepen the understanding of the relationship between soil properties and agricultural tillage practices.

TABLE I
SUMMARY OF PLOT CHARACTERISTICS FROM GROUND MEASUREMENTS

Plot	Crop type	Tillage practices	Ridge period / height	Registration error（cm）
#117	Corn	Plowing	—	0.56
#81	Corn	Harrowing	—	0.89
#102	Corn	Ridging	105 cm / 12.6 cm	0.56
#106	Soybeans	Crusting	104 cm / 8.3 cm	0.6
#D20	Soybeans	Harrowing	—	0.64
#99	Soybeans	Ridging	104 cm / 14.7 cm	0.52

II. MATERIALS AND METHODS

A. Experiments

Friendship farm (FF) is a modern agricultural experimental area located in the southeast of Heilongjiang Province, China. It is the largest mechanized state-owned farm in China, primarily cultivating crops like corn, soybeans, and rice. FF is considered representative of the agricultural areas in Northeast China, with an average elevation of 78 m. The terrain is mainly plain, the soil type is black soil, and the annual precipitation is about 514 mm.

In FF, a 54 km $\times$ 32 km area was selected as the research area (see Fig. 1), including corn fields, soybean fields, and rice fields. In October 2022, a multisource remote sensing monitoring experiment involving satellite, aircraft, and ground components was conducted at FF. In this experiment, TLS was used to measure the SSR of six different farmland plots (combinations of different tillage practices and crop types), and corresponding basic data such as surface soil moisture, ridge direction, and ridge structure were obtained. Fields #117, #81, and #102 are corn fields, while #106, #D20, and #99 are soybean fields. Field #117 underwent plowed treatment. Fields #102 and #99 were subjected to ridged treatment, whereas #81 and #D20 received harrowed treatment. Field #106 was in a crusted state. Detailed information about the measured fields can be found in Table I.

B. Point Cloud Measurement Based on TLS and Data Preprocessing

All farm plots were scanned using the Trimble TX8 TLS. This device has an effective scanning range of 0.6 to 120 m and ensures scanning accuracy of less than 1 mm. When scanning a

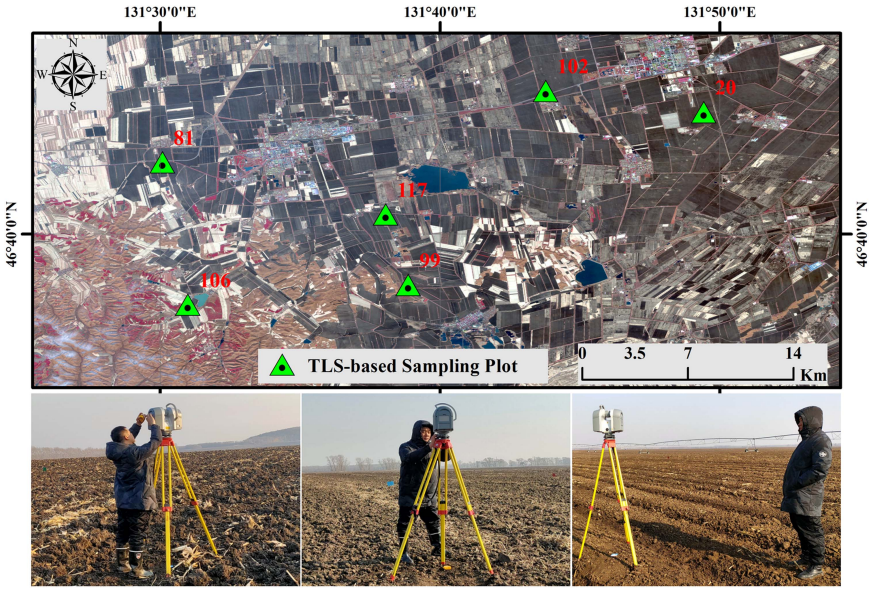

Fig. 1. Geographic location of the research area and distribution of six agricultural field sample plots based on Sentinel-2 false-color imagery. Photographs of the field measurement work for plots #117, #D20, and #102 are displayed at the bottom.

plot, the scanning radius was set at 25 m with a point spacing of about 5.7 mm. The device's horizontal field of view covers 0°–360°, while the zenith field of view is between 30° and 130°. As the scanning distance increases, the point cloud density gradually decreases. To obtain a sufficiently dense point cloud within the measurement area, scanning is typically carried out at four different positions to cover the 25 m × 25 m farm soil surface [31]. Furthermore, all four scanning positions are located using the global positioning system to ensure high-precision geographical location information for the measured point clouds.

For each plot, the iterative closest point algorithm was used to register point cloud data from the four sites [25], [32]. Subsequently, moving least squares was applied to remove point cloud noise that might affect soil surface elevation information, thereby smoothing the point cloud data. To facilitate the calculation of SSR and reduce computational resource consumption, we used ArcGIS 10.8 software to perform bilinear interpolation on the preprocessed point cloud data, generating a digital elevation model (DEM) for each plot. Considering the SSR measurement requirements, we set the interpolated DEM's spatial resolution to 1 cm [7]. The Hodrick–Prescott filter was used to remove the trend component from each profile (25 m) to eliminate the influence of local terrain slope (see Fig. 2).

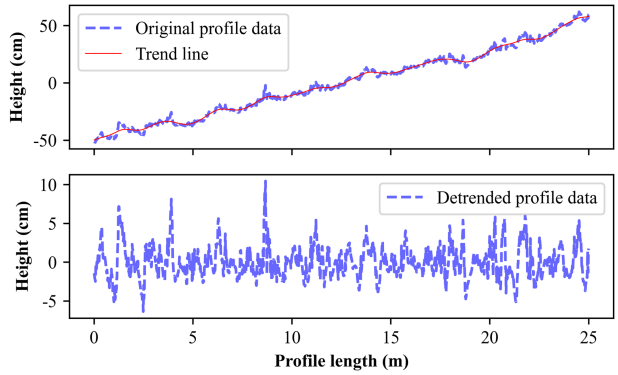

Fig. 2. Comparison of soil profile data before and after detrending. The harrowed plot (#81) is displayed in the 25-m profile data at 30°.

C. Surface Roughness Parameters Calculation

The RMSH and CL of the random rough surface quantitatively describe the SSR in the vertical and horizontal directions, respectively. These are two key parameters for analyzing fluctuations in random surface heights. The RMSH [7] is defined as

$$\mathrm{RMSH} = \sqrt{\frac{1}{N}\sum_{i=1}^{N}\left(Z_i - \bar{Z}\right)^2} \tag{1}$$

where N is the number of samples on each profile length. Z_i is the surface height corresponding to record i. $\bar{Z}$ is the average height of Z_i over the profile length.

When calculating the CL, the experimental ACF of each independent profile length is first computed based on each profile [7], [33]

$$R(h) = \sum_{i=1}^{N(h)} Z_i Z_{i+h} \Big/ \sum_{i=1}^{N} {Z_i}^2 \tag{2}$$

where $R(h)$ represents the experimental ACF at lag h, describing the correlation between two points at a horizontal distance and their surface elevations. $N(h)$ is the number of pairs considered in each lag h. Z_{i+h} is the height of another point located at a lag distance h from it (Z_i).

Then, the theoretical ACF ($C(h)$) is chosen to fit the experimental ACF ($R(h)$)

$$C(h) = \exp(-(h/cl)^n). \tag{3}$$

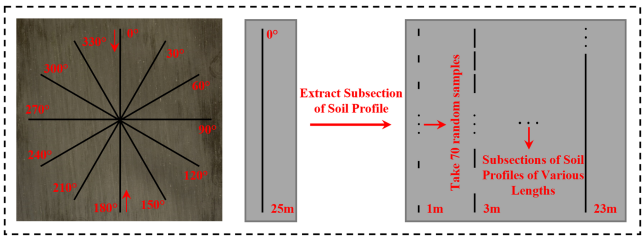

Fig. 3. Schematic diagram for extracting subprofiles from a 25-m profile data.

$n = 1$ (and 2) denotes the exponential (and Gaussian) function. when $C(h)$ equals $1/e$, the distance (h) between these two points is the CL.

In this study, based on the due north direction, 25 m soil profiles were extracted from the 25 m×25 m plot's DEM at 30° intervals clockwise (a total of 12 directions). To analyze the impact of profile length on roughness parameters, 12 subprofiles (1, 3, 5, …, 21, 23 m) were obtained from the detrended 25-m soil profile data in each direction (see Fig. 3). Here, 1 m serves as the minimum subprofile length, with subsequent subprofiles acquired at 2 m intervals. Each subprofile data were sampled 70 times at random within the 25 m profile, and the average SSR was taken as the measurement value of that subprofile data.

In this study, the average RMSH (CL) over all directions of the 25-m profile length was taken as the "true" SSR value of the plot. Detailed results can be seen in Section III-A.

III. Results

A. Point Cloud and DEM Measurement Results

Fig. 4 shows the elevation fluctuation characteristics of farmland under different crop types and tillage practices, which are closely related to SSR. Through such analysis, we can better understand the characteristics of SSR under different tillage practices. The left picture (first column) shows the on-site photos of different plots, each with different agricultural tillage practices at the same period. The second column is a point cloud map of farmland surface elevation obtained with TLS, representing the three-dimensional structure of the farmland terrain. The change in colors indicates different heights on the farmland surface. Colors transition from blue to red, representing the change from low to high points. The third column is a DEM map based on point cloud data, representing the degree of high and low undulations in the farmland terrain. By comparing the degree of color change in the point cloud map and DEM map, it can be intuitively seen that the DEM map can better restore the point cloud data's description of the differences in farmland surface elevation.

The right picture is the elevation cumulative probability diagrams of different plots, with curves in the graph showing how ground height variations are distributed throughout the plot. The blue (red) line represents the elevation statistical distribution of the point cloud (DEM) data. By comparison, it is found that the elevation cumulative probability curves of point cloud data and DEM data are basically consistent. The steeper the curve, the more concentrated the elevation change. The elevation change of the plots in this study is mainly concentrated between -0.1 and 0.1 m.

In addition, we calculated the SSR of different plots, including RMSH and CL (exponential and Gaussian forms) (see Fig. 5). The average SSR obtained from the 25-m profile data of each plot (including 12 orientations) was used as the overall SSR of the entire plot. Fig. 5(a) shows the RMSH of six typical plots. Among the corn plots, the plowed plot (#117) showed the greatest vertical roughness, with an RMSH of 2.49 cm. This was followed by the ridged plot (#102) (RMSH: 2.02 cm). The harrowed plot (#81) showed a smaller RMSH (1.81 cm) compared to the first two types of plots. Among the soybean plots, the crusted (#106) and ridged (#99) plots exhibited similar RMSH (2.07 and 2.15 cm, respectively). The harrowed plot (#D20) had the smallest RMSH (1.5 cm). Fig. 5(b) shows the CL in exponential form, describing the characteristics of SSR in the horizontal direction. Among the corn plots, the ridged plot (#102) had the longest CL (15.42 cm). The harrowed plot (#81) had the shortest CL (9.63 cm). The soybean plots showed the same conclusion, with the ridged (#99) and harrowed (#D20) plots having the longest (14.48 cm) and shortest (5.93 cm) CL, respectively. In addition, a similar pattern was found for exponential- and Gaussian-based CL among different tillage practices [see Fig. 5(b) and (c)]. The maximum RMSH produced by the plowed plot (#117) and the minimum RMSH produced by the harrowed plot (#D20) had a difference of 0.98 cm, with a ratio of 1.65 times. CL is more affected by different tillage methods than RMSH. For example, the maximum CL in exponential form (15.42 cm) caused by the ridged plot (#102) compared to the minimum CL in exponential form (5.93 cm) corresponding to the harrowed plot (#D20) had a difference of 9.49 cm, with the ratio reaching as high as 2.6 times.

Overall, RMSH and CL provided us with the characteristics of farmland SSR in the vertical and horizontal directions under different tillage practices. Plowed plots produce higher RMSH, and the CL value is relatively higher as well. Ridged plots lead to higher CL in farmlands. Harrowed plots, by breaking up the soil blocks, result in smaller RMSH and CL values for farmland roughness.

B. Anisotropy of SSR Under Different Agricultural Tillage Practices

In this study, RMSH and CL for the 25-m profile length data were calculated corresponding to different azimuth angles. Fig. 6 displays the variation of RMSH and CL (exponential form) under different azimuth angles for farmland plots with different agricultural tillage practices. In addition, Table II lists the average value, standard deviation (SD), and the ratio of the maximum to minimum value (referred to as RMM) of RMSH or CL between different azimuth angles of the plots.

The SSR of corn plots revealed that the plowed plot (#117) had higher average RMSH (2.49 cm) and SD (0.31 cm), indicating significant unevenness and variability of the soil surface after plowing. This is consistent with spikes in certain directions [see Fig. 6(a)], such as 90°, 150°, and 180°. Harrowed plot (#81) showed lower average RMSH (1.81 cm) and SD (0.15 cm),

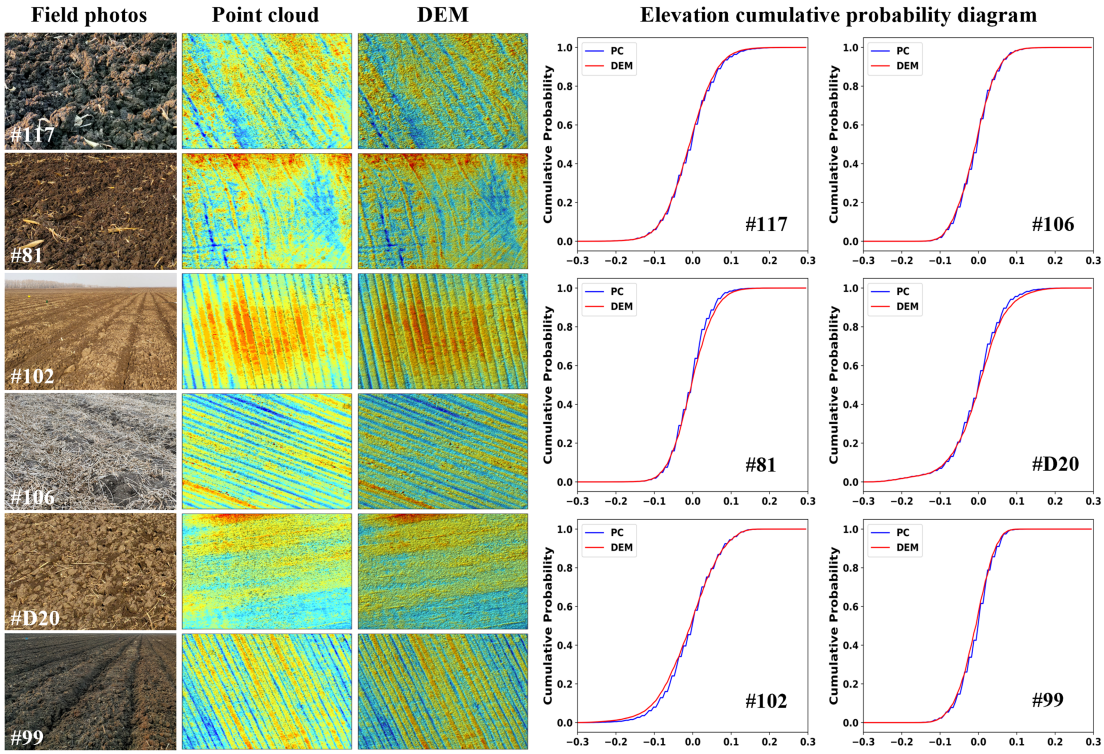

Fig. 4. Field images of agricultural plots, point cloud maps, and DEM maps (left image). Elevation cumulative probability diagrams of different plots (right image).

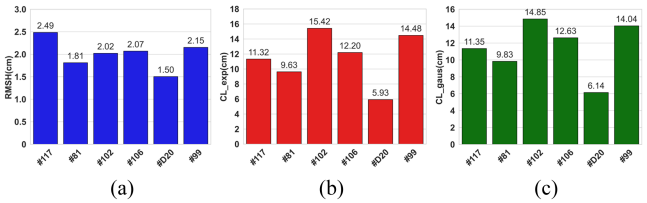

Fig. 5. SSR estimation for six 25 m × 25 m plots. (a) RMSH. (b) CL based on exponential function. (c) CL based on Gaussian function.

suggesting a flatter and more uniform soil surface. The relatively uniform distribution of RMSH and CL in different directions on the radar chart also reflects this characteristic. Ridged plot (#102) exhibited high SD (0.73 and 4.76 cm) and RMM (2.99 and 2.93) for RMSH and CL, indicating significant SSR parameter variation with direction. This suggests that ridging leads to significant height and structural variability of the soil surface, closely related to the direction of the ridges.

The SSR of soybean plots showed that the crusted plot with ridges (#106) had moderate SD (0.43 cm) and RMM (1.83) for RMSH, indicating some unevenness of the soil surface. The peak near the 150° azimuth in Fig. 6(g) may be due to the ridge structure. The soybean fields are structured with ridges using agricultural machinery before planting. Although the ridge structure evolves over time and with factors like rainfall events, postharvest soybean fields still exhibit some ridge structure, which could impact the measurement of field SSR. Harrowed plot (#D20) had low average RMSH (1.5 cm) and SD (0.18 cm), indicating a more uniform soil surface, similar to corn plot (#81), reflecting the flattening effect of harrowing on the soil (or soil clods) surface. Ridged plot (#99) exhibited high RMM (2.42 and 2.08) for RMSH and CL, with significant SSR variation in certain directions, indicating ridging caused distinct SSR characteristics in some directions.

Overall, harrowing (#81 and #D20) typically results in a flatter and more uniform soil surface, with lower average RMSH ($\leq$ 1.81 cm) and SD ($\leq$ 0.18 cm). The RMM of RMSH (1.3 and 1.47) is less than the average RMM of RMSH for all plots (1.9). The SSR anisotropy of the harrowed plot can be disregarded. Ridging (#102 and #99) and crusting (#106) caused significant directional variation in SSR, as shown by the higher SD ($\leq$ 0.73 and 4.76 cm) and RMM ($\leq$ 2.99 and 2.93) for RMSH and CL. Plowing (#117) caused significant changes in soil surface height, reflected in the higher average RMSH (2.49 cm). However, directional anisotropy is not pronounced.

C. Measurement Requirements for SSR Under Different Agricultural Tillage Practices

Fig. 7 indicates that a 1-m profile length corresponds to a larger measurement error for RMSH and CL. Moreover, most plots showed a trend of reduced variability in RMSH and CL with increasing profile length, possibly because longer profiles better represent the overall characteristics of the soil surface, reducing the impact of local heterogeneity. The median range of RMSH was relatively stable across the six plots with increasing

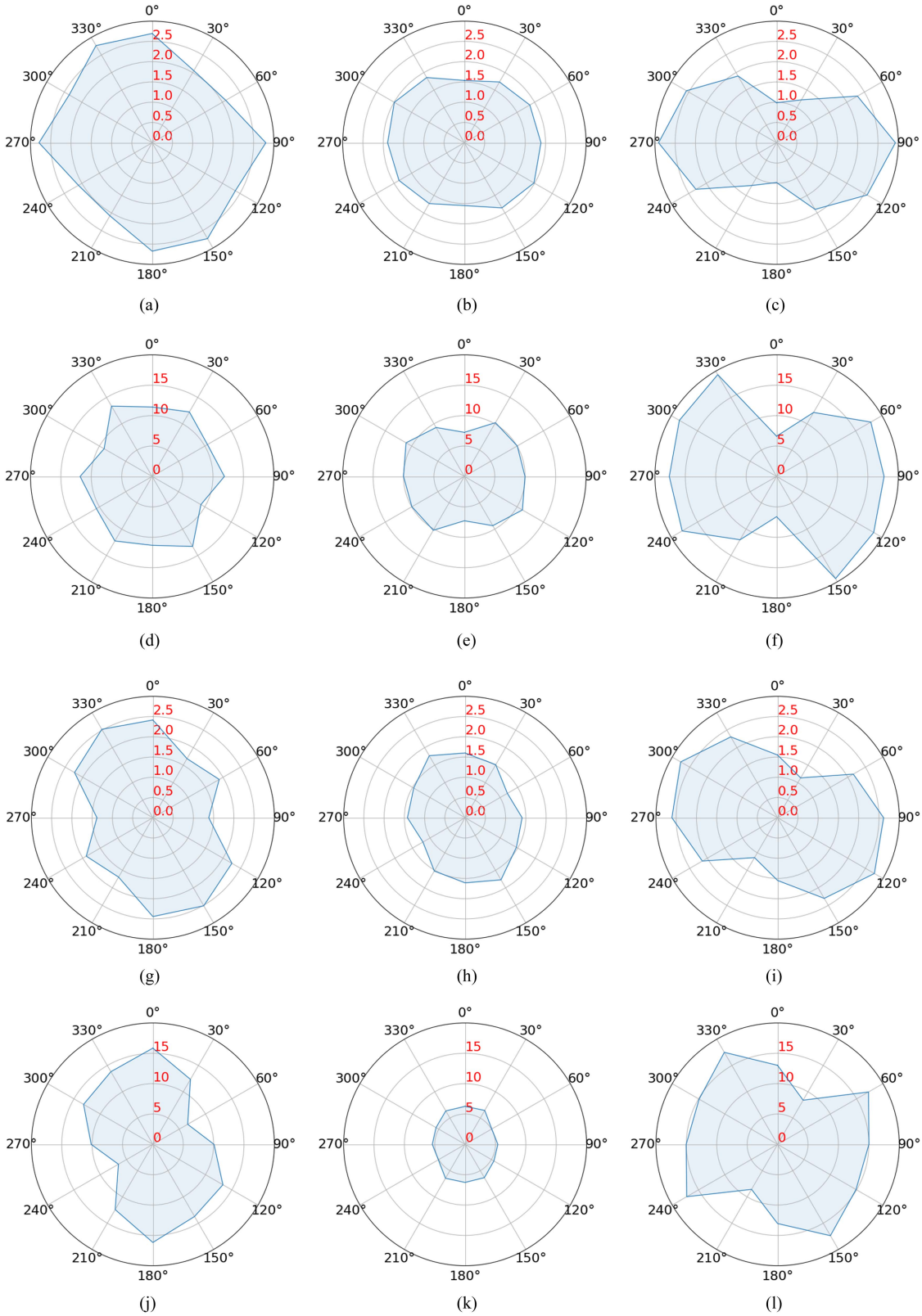

Fig. 6. Anisotropy in RMSH and CL with a profile length of 25 m. RMSH: (a), (b), (c), (g), (h), and (i). CL: (d), (e), (f), (j), (k), and (l).

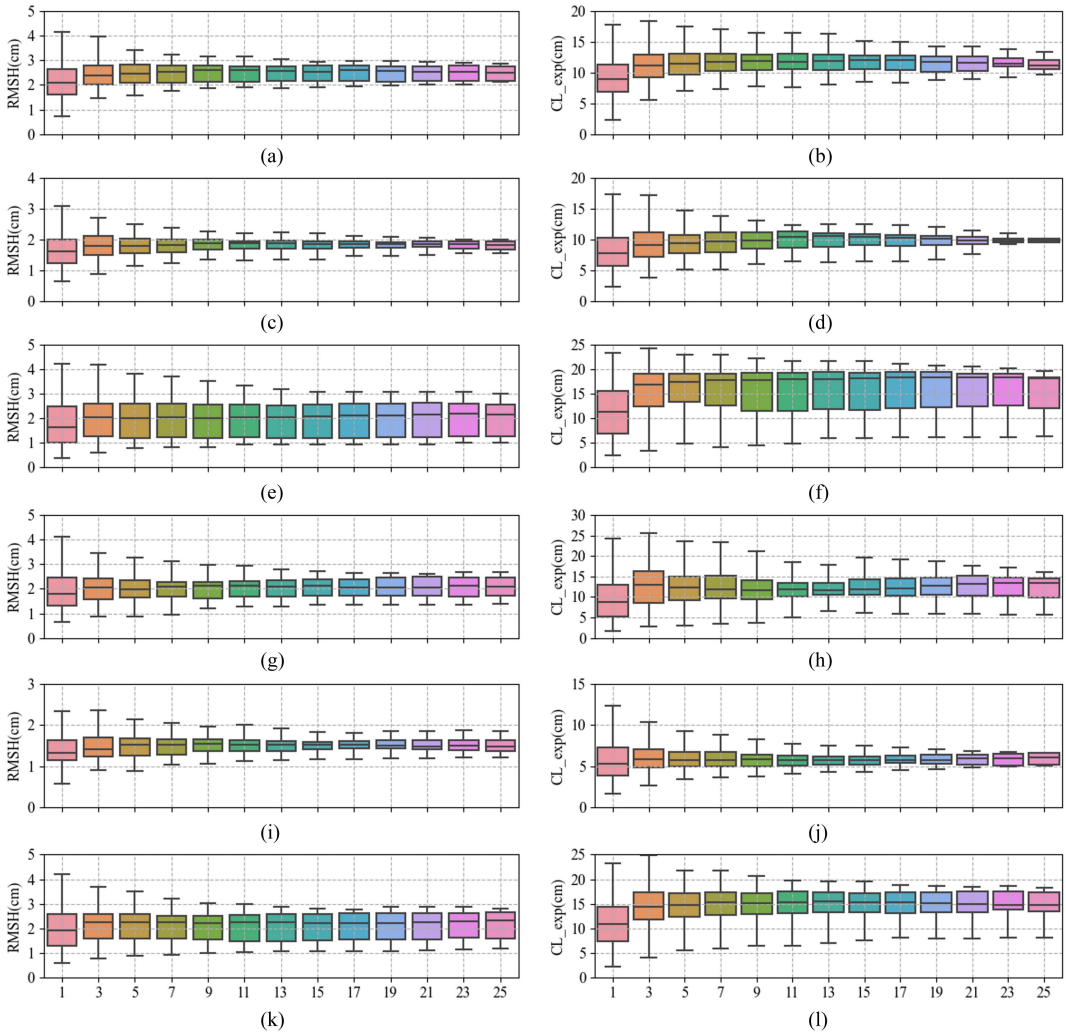

Fig. 7. Box plots of RMSH (left panel) and CL (right panel) with different profile lengths. Each profile length corresponds to 12 directions × 70 random repeated measurements (a total of 840 sets). (a) and (b): #117. (c) and (d): #81. (e) and (f): #102. (g) and (h): #106. (i) and (j): #D20. (k) and (l): #99.

profile length. The median distribution of CL generally increased with profile length, especially on plots #102 [see Fig. 7(f)] and #99 [see Fig. 7(l)], indicating that longer profiles reveal longer spatial correlations. In addition, the study analyzed the impact of different agricultural tillage practices on the accuracy of SSR measurements. Plots with plowing treatment [#117, Fig. 7(a)] appeared to have greater variability in RMSH, possibly due to the plowing making the soil surface rougher. Harrowed plots [#81, Fig. 7(c) and #D20, Fig. 7(i)] exhibited smaller SSR and more stable RMSH distributions. Ridged plots [#102, Fig. 7(f) and #99, Fig. 7(l)] showed a more pronounced growth trend in CL, possibly because ridging created periodic soil structures more easily observed over longer profile lengths.

For farmland under different agricultural tillage practices, this study analyzed how long the sampling profile length needs to be to accurately obtain SSR (RMSH and CL). Figs. 8 and 9 present the average values of RMSH (and CL) calculated using different profile lengths. It is worth noting that the SSR value for each profile length is the average of 12 directions × 70 repeated measurements (a total of 840 sets). The red dashed line is the RMSH at a 25-m profile length as the reference value for the entire plot. The green (blue) dashed lines are the 5% error upper (lower) limits of the 25-m profile length RMSH (and CL). The results suggest that a profile length of at least 3 m is needed to ensure that the measured RMSH (and CL) has an error better than 5% relative to the plot reference value. For plowed [see Fig. 8(a)] and harrowed plots [see Fig. 8(b) and (e)], the RMSH values at a 3-m profile length already had a small error relative to the reference value, and increasing the profile length did not significantly reduce the error. For crusted [see Fig. 8(d)] and ridged plots [see Fig. 8(c) and (f)], the error between the RMSH values at different profile lengths and the reference value fluctuated more. Overall, as the profile length increased, the error between the measured values and the reference value decreased. This is because the crusted and ridged plots in this study have periodic structures and longer profile length measurements better represent the elevation fluctuation characteristics of the plot. At a 1-m profile length, CL measurements exhibited greater uncertainty, especially for crusted and ridged plots. When the profile length measurement exceeded 3 m, CL measurements

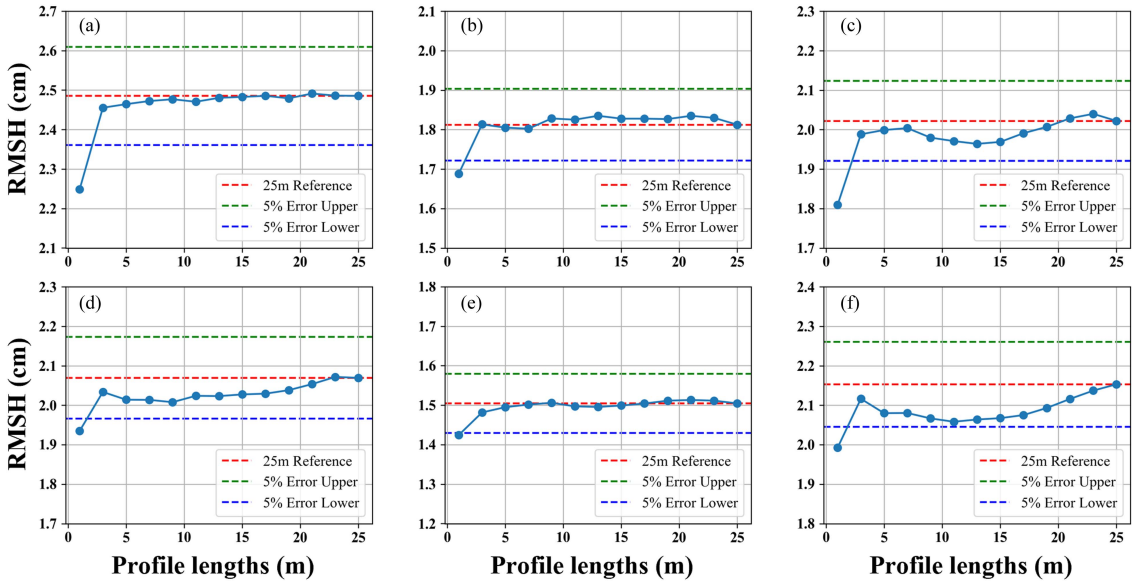

Fig. 8. Measurement accuracy of RMSH varies with different profile length. Plowing: #117. Harrowing: #81 and #D20. Ridging: #102 and #99. Crusting (with ridge): #106.

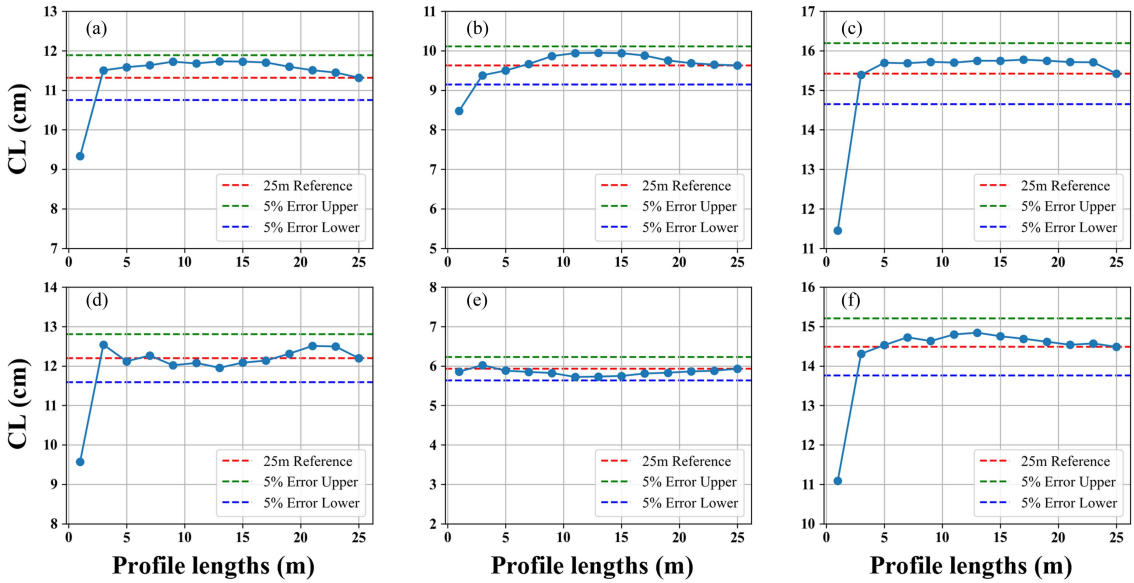

Fig. 9. Measurement accuracy of CL varies with different profile length. Plowing: #117. Harrowing: #81 and #D20. Ridging: #102 and #99. Crusting (with ridge): #106.

fluctuated around the reference value but met the 5% error accuracy requirement for CL measurements. Therefore, when using TLS to measure the SSR of farmland under different agricultural tillage practices, a measurement range of at least 3 m $\times$ 3 m should be ensured.

IV. Discussion

A. How Do Different Agricultural Tillage Practices Affect SSR?

Soil tillage, a necessary measure in crop production, affects soil's physical properties crucial for plant growth, such as soil porosity, permeability, and SSR [34]. Different agricultural tillage practices impact farmland SSR because these practices change the soil's physical structure and surface characteristics. Traditional tillage in the Northeast black soil agricultural area mainly includes plowing, harrowing, and ridging. Plowing usually involves using a plow to turn and break up the soil. This increases SSR due to the upturned soil clods and furrows changing the soil surface's uniformity. Harrowing is used to further refine soil particles, usually performed after plowing. It can reduce SSR by helping to flatten the soil and reduce large clods. Ridging creates ridges and furrows between rows, significantly increasing SSR. The ridged soil surface becomes uneven due to the shape of the ridges and furrows. In addition, the surface state of the soil after crop harvesting and before

TABLE II
STATISTICAL INDICATORS OF SSR FOR DIFFERENT PLOTS

Plot	Statistical Indicators	RMSH (cm)	CL_exp (cm)	CL_gaus (cm)
#117	Average	2.49	11.32	11.35
	SD	0.31	1.37	1.32
	RMM	1.36	1.46	1.45
#81	Average	1.81	9.63	9.83
	SD	0.15	1.22	1.19
	RMM	1.30	1.53	1.48
#102	Average	2.02	15.42	14.85
	SD	0.73	4.76	4.25
	RMM	2.99	2.93	2.76
#106	Average	2.07	12.20	12.63
	SD	0.43	3.13	3.16
	RMM	1.83	2.47	2.46
#D20	Average	1.50	5.93	6.14
	SD	0.18	0.56	0.59
	RMM	1.47	1.27	1.29
#99	Average	2.15	14.48	14.04
	SD	0.60	3.16	2.76
	RMM	2.42	2.08	1.92
ALL	Average	2.01	11.50	11.47
	SD	0.40	2.37	2.21
	RMM	1.90	1.96	1.89

any mechanized treatment is referred to as "crusting." Crusting refers to a tight, hardened layer formed on the soil surface, typically caused by rain impact and subsequent drying. This phenomenon might decrease roughness, as the crusted surface is smoother than uncrusted soil. However, due to the influence of periodic structures, crusted surfaces with ridge structures might have higher roughness values.

Different soil tillage practices result in a combination of directional, periodic structures and uncertain random variations for SSR in three-dimensional space, posing significant challenges to SSR measurement. For instance, when ridges and furrows are well developed, SSR measurements are highly sensitive to the orientation of the profile relative to the tillage structure. This sensitivity is particularly severe in CL measurements. For farmland with ridge structures, measurements parallel to the ridges mainly reflect the random components of SSR. When measured perpendicular to the rows, the periodic characteristics introduced by the rows should be removed from the obtained SSR profiles and considered separately in the modeling of microwave remote sensing's backscatter coefficient [35].

B. Relationship Between RMSH and CL Under Different Agricultural Tillage Practices

This study analyzed the linear relationship between RMSH and CL under different tillage practices (see Fig. 10). SSR of each plot in 12 azimuth directions (considering only 25-m profile length) was included in the analysis. The results show ridged plots (#99 and #102) cause a wide range of RMSH and CL values. Plowed plot (#117) results in generally higher RMSH values. Harrowed plots (#D20 and #81) have lower RMSH

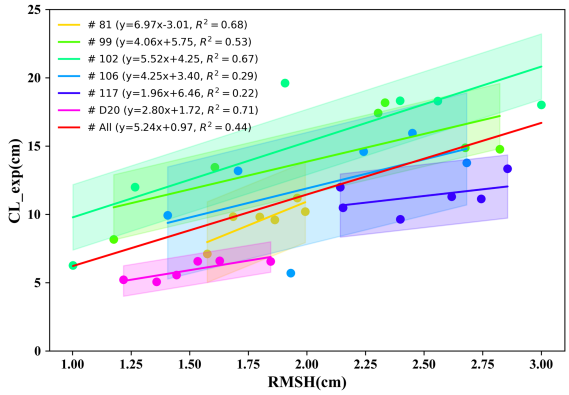

Fig. 10. Relationship between RMSH and CL under different agricultural tillage practices. Plowing: #117. Harrowing: #81 and #D20. Ridging: #102 and #99. Crusting (with ridges): #106. The lines in the figure represent the trend lines of the scatter plot of RMSH and CL for different plots and are marked with the corresponding fitting formula and R^2 in the legend. Note that the red line represents the trend line for all plots. Different colored filled areas for each type of plot indicate the confidence interval of the trend line.

values. Crusted plot (#106), due to the residual ridge structure, still has a wide fluctuation range of RMSH and CL.

The differences in R^2 values between plots with different tillage practices may indicate the varying impacts of these treatments on soil properties. The trend lines and R^2 of the relationship between RMSH and CL for plots with different agricultural tillage practices were calculated and analyzed. The results show a positive linear correlation between RMSH and CL in different agricultural tillage practices. The R^2 between RMSH and CL for all plots is 0.44. Different agricultural tillage practices significantly affect the relationship between RMSH and CL. The linear explanatory degree of the relationship between RMSH and CL is highest in harrowed plots, with $R^2 \geq 0.68$. Next are the ridged plots ($R^2 \geq 0.53$). The plowed plot has the poorest fit of RMSH and CL, with $R^2 = 0.22$. This may be due to the severe disruption of soil structure by plowing, affecting the relationship between RMSH and CL. Although different tillage practices affect the specific relationship between RMSH and CL, the overall trend line and higher R^2 values for all plots provide a comprehensive perspective, generally showing a positive linear correlation.

C. Prospects for Measuring SSR Under Different Agricultural Tillage Practices

As agricultural production practices evolve, farming practices exhibit diverse characteristics, including traditional, conservative, and organic tillage. Traditional tillage typically involves plowing and harrowing with tools like plows and harrows, which help to loosen the soil and facilitate seed sowing. However, frequent soil tillage may lead to increased soil roughness, destruction of soil structure, loss of organic matter, and soil and water erosion [20]. In some traditional agricultural areas, traditional tillage remains widespread. Conservative tillage includes practices such as no-till and reduced-till, aimed at reducing soil disturbance, leading to different soil structures and SSR. These practices are particularly popular in arid or semiarid

regions because they help to reduce erosion and improve water retention capabilities [30]. In addition, conservative tillage includes returning crop straw to the field, and the crop straw cover on the soil surface also affects SSR measurements. Each tillage practice has a different impact on soil structure and SSR. Soil structure and SSR parameters significantly influence the radiation or reflection of electromagnetic waves in microwave remote sensing. For example, the direction of tillage rows and whether the field has been plowed have a significant impact on the microwave remote sensing inversion of surface soil moisture. Therefore, identifying the direction of ridges and the plowing status of fields through optical or microwave remote sensing means is crucial for accurately generating large-area, bare SSR of farmland [14]. In addition, future investigations of SSR should include more detailed periodic roughness components. This is beneficial for quantifying the contribution of periodic components in microwave remote sensing backscatter modeling [36].

With the development of sensors and sensor platforms, SSR measurement has evolved from early contact methods (pin profilometers) to modern noncontact techniques such as optical measurements and LiDAR. Optical measurements utilize high-resolution cameras and image processing software for SSR analysis. LiDAR employs laser scanning to capture three-dimensional data of surfaces. For instance, one of the main advantages of TLS in characterizing SSR is its three-dimensional measurement capability. Using TLS data, the SSR in any direction for any point within an effective area can be calculated. TLS can replace pin profilometers for characterizing SSR. Moreover, TLS allows for the parameterization of SSR on a three-dimensional scale [23]. This method offers higher measurement precision and efficiency, especially effective in large-scale and complex terrain measurements.

There are two main trends in the forefront of using LiDAR scanning for farmland SSR measurement: miniaturization and portability, and commercialization and large-scale application. For example, integrating LiDAR into smartphones makes the device not only portable but also easy to operate. This approach enables farmers and researchers to measure farmland SSR precisely and conveniently. However, the challenge with such miniaturized devices is ensuring measurement accuracy and range. On the other hand, utilizing LiDAR on spacecraft or satellites for large-scale farmland SSR measurement can provide large-scale data, which is very useful for regional studies and long-term monitoring. The current challenge is improving the resolution of LiDAR on these platforms to meet the needs for precise farmland SSR measurement. Addressing this issue may require higher technological innovation, such as improving LiDAR scanning techniques or adopting more advanced data processing methods to enhance resolution.

However, current SSR measurement technologies face challenges in very dense vegetation areas, as imaging the soil surface becomes difficult. In such situations, developing more advanced imaging techniques (such as multiwavelength and multiangle imaging) and utilizing advanced data processing algorithms to separate vegetation and ground surface information emerges as a solution. In addition, employing machine learning and artificial intelligence algorithms to analyze complex datasets, thereby inferring SSR in vegetated areas, represent a potential research direction. The development of these technologies will enable the measurement of SSR in areas with dense vegetation.

V. Conclusion

Farmland SSR is a significant influencing factor in soil erosion, soil moisture distribution, and soil nutrient transport. Tillage activities have led to increased instability in farmland SSR. This study used TLS to measure the SSR of six farmland plots (combinations of different tillage practices and crop types) in the black soil region of Northeast China and analyzes the characteristics of farmland SSR under different agricultural tillage practices (plowing, harrowing, ridging, crusting, etc.). The study shows the following results.

1) Different agricultural tillage practices result in significant differences in the farmland SSR. The plowed (#117) and harrowed plot (#D20) correspond to the maximum (2.49 cm) and minimum (1.5 cm) RMSH, respectively. The difference in their RMSH is 0.98 cm, with a ratio of 1.65 times. CL is more affected by different tillage practices than RMSH. The maximum (15.42 cm) and minimum (5.93 cm) CL differ by 9.49 cm, with a ratio of 2.6 times, corresponding to the ridged plot and the harrowed plot, respectively.
2) Ridging and crusting caused significant directional variation in SSR, as shown by the higher SD ($\leq$ 0.73 and 4.76 cm) and RMM ($\leq$ 2.99 and 2.93) for RMSH and CL. The SSR anisotropy of the harrowed plot can be disregarded.
3) Under the condition of measuring soil profile in 12 directions and randomly sampling 70 times in each direction, the profile length must be at least 3 m to ensure that the measurement error of SSR (RMSH and CL) is better than 5% compared to the "true" value. TLS can measure two-dimensional SSR. Therefore, it is only necessary to ensure that the measurement range is at least 3 m $\times$ 3 m. These conclusions help to understand the impact of different agricultural tillage practices on SSR, providing references for agricultural production practices, soil erosion modeling, and microwave remote sensing inversion of soil moisture.

References

[1] F. Darboux et al., "Evolution of soil surface roughness and flowpath connectivity in overland flow experiments," *Catena*, vol. 46, no. 2–3, pp. 125–139, Jan. 2002.
[2] C. H. Huang and J. M. Bradford, "Applications of a laser scanner to quantify soil microtopography," *Soil Sci. Soc. Amer. J.*, vol. 56, no. 1, pp. 14–21, Jan./Feb. 1992.
[3] B. Sharratt and G. L. Feng, "Friction velocity and aerodynamic roughness of conventional and undercutter tillage within the Columbia Plateau, USA," *Soil Tillage Res.*, vol. 105, no. 2, pp. 236–241, Nov. 2009.
[4] X. M. Zheng et al., "Simultaneously estimating surface soil moisture and roughness of bare soils by combining optical and radar data," *Int. J. Appl. Earth Observ. Geoinf.*, vol. 100, pp. 102345, Aug. 2021.
[5] N. E. C. Verhoest et al., "On the soil roughness parameterization problem in soil moisture retrieval of bare surfaces from synthetic aperture radar," *Sensors*, vol. 8, no. 7, pp. 4213–4248, Jul. 2008.

[6] L. J. Zhu and G. H. Zhang, "Review of measurement and quantification of surface microtopography," *Sci. Soil Water Conservation*, vol. 11, no. 05, pp. 114–122, Oct. 2013.
[7] X. M. Zheng et al., "Measuring surface roughness of agricultural soils: Measurement error evaluation and random components separation," *Geoderma*, vol. 404, pp. 115393, Dec. 2021.
[8] F. T. Ulaby, A. Aslam, and M. C. Dobson, "Effects of vegetation cover on the radar sensitivity to soil-moisture," *IEEE Trans. Geosci. Remote Sens.*, vol. GE-20, no. 4, pp. 476–481, Oct. 1982.
[9] X. Blaes and P. Defourny, "Characterizing bidimensional roughness of agricultural soil surfaces for SAR modeling," *IEEE Trans. Geosci. Remote Sens.*, vol. 46, no. 12, pp. 4050–4061, Dec. 2008.
[10] L. Li, X. Zheng, X. Li, X. Li, T. Jiang, and X. Wan, "Potential and accurate evaluation of unmanned aerial vehicle remote sensing for soil surface roughness measurement," *IEEE J. Sel. Topics Appl. Earth Observ. Remote Sens.*, vol. 14, pp. 7961–7967, 2021.
[11] X. M. Zheng et al., "The temporal variation of farmland soil surface roughness with various initial surface states under natural rainfall conditions," *Soil Tillage Res.*, vol. 170, pp. 147–156, Jul. 2017.
[12] Z. Alijani et al., "Sensitivity of C-band SAR polarimetric variables to the directionality of surface roughness parameters," *Remote Sens.*, vol. 13, no. 11, pp. 2210, Jun. 2021.
[13] J. C. Landy, D. Isleifson, A. S. Komarov, and D. G. Barber, "Parameterization of centimeter-scale sea ice surface roughness using terrestrial LiDAR," *IEEE Trans. Geosci. Remote Sens.*, vol. 53, no. 3, pp. 1271–1286, Mar. 2015.
[14] R. Turner et al., "Estimation of soil surface roughness of agricultural soils using airborne LiDAR," *Remote Sens. Environ.*, vol. 140, pp. 107–117, Jan. 2014.
[15] L. M. Thomsen et al., "Soil surface roughness: Comparing old and new measuring methods and application in a soil erosion model," *Soil*, vol. 1, no. 1, pp. 399–410, 2015.
[16] Z. Alijani et al., "A comparison of three surface roughness characterization techniques: Photogrammetry, pin profiler, and smartphone-based LiDAR," *Int. J. Digit. Earth*, vol. 15, no. 1, pp. 2422–2439, 2022.
[17] M. Chabot et al., "Comparing the use of terrestrial LiDAR scanners and pin profilers for deriving agricultural roughness statistics," *Can. J. Remote Sens.*, vol. 44, no. 2, pp. 153–168, 2018.
[18] A. Martinez-Agirre et al., "Evaluation of terrestrial laser scanner and structure from motion photogrammetry techniques for quantifying soil surface roughness parameters over agricultural soils," *Earth Surf. Processes Landforms*, vol. 45, no. 3, pp. 605–621, Mar. 2020.
[19] F. Mattia et al., "A comparison between soil roughness statistics used in surface scattering models derived from mechanical and laser profilers," *IEEE Trans. Geosci. Remote Sens.*, vol. 41, no. 7, pp. 1659–1671, Jul. 2003.
[20] I. J. Davenport, N. Holden, and R. J. Gurney, "Characterizing errors in airborne laser altimetry data to extract soil roughness," *IEEE Trans. Geosci. Remote Sens.*, vol. 42, no. 10, pp. 2130–2141, Oct. 2004.
[21] S. N. Haubrock et al., "Spatiotemporal variations of soil surface roughness from in-situ laser scanning," *Catena*, vol. 79, no. 2, pp. 128–139, Nov. 2009.
[22] M. Hollaus et al., "Roughness mapping on various vertical scales based on full-waveform airborne laser scanning data," *Remote Sens.*, vol. 3, no. 3, pp. 503–523, Mar. 2011.
[23] W. Ni, G. Sun, Z. Guo, and Y. Pang, "Characterization of soil surface roughness from terrestrial laser scanner data," in *Proc. IEEE Int. Symp. Geosci. Remote Sens.*, 2009, pp. II–428–II–431.
[24] C. F. Chen and T. X. Yue, "A method of DEM construction and related error analysis," *Comput. Geosciences*, vol. 36, no. 6, pp. 717–725, Jun. 2010.
[25] L. Li et al., "The effects of DEM interpolation on quantifying soil surface roughness using terrestrial LiDAR," *Soil Tillage Res.*, vol. 198, pp. 104520, Apr. 2020.
[26] A. Martinez-Agirre, J. Álvarez-Mozos, H. Lievens, and N. E. C. Verhoest, "Influence of surface roughness measurement scale on radar backscattering in different agricultural soils," *IEEE Trans. Geosci. Remote Sens.*, vol. 55, no. 10, pp. 5925–5936, Oct. 2017.
[27] X. M. Zheng, K. Zhao, and X. J. Li, "Accuracy analysis of agriculture soil surface roughness parameter," *J. Geo-Inf. Sci.*, vol. 15, no. 05, pp. 752–760, 2013.
[28] R. Bryant et al., "Measuring surface roughness height to parameterize radar backscatter models for retrieval of surface soil moisture," *IEEE Geosci. Remote Sens. Lett.*, vol. 4, no. 1, pp. 137–141, Jan. 2007.
[29] H. J. Zhang and Y. R. Sun, "Soil surface roughness indices, interpretation and application," *Trans. Chin. Soc. Agricultural Machinery*, vol. 41, no. 03, pp. 33–39, Mar. 2010.
[30] C. M. Pittelkow et al., "Productivity limits and potentials of the principles of conservation agriculture," *Nature*, vol. 517, no. 7534, pp. 365–U482, Jan. 2015.
[31] Y. Oh and Y. C. Kay, "Condition for precise measurement of soil surface roughness," *IEEE Trans. Geosci. Remote Sens.*, vol. 36, no. 2, pp. 691–695, Mar. 1998.
[32] P. J. Besl and N. D. McKay, "A method for registration of 3-D shapes," *IEEE Trans. Pattern Anal. Mach. Intell.*, vol. 14, no. 2, pp. 239–256, Feb. 1992.
[33] F. T. Ulaby et al., *Microwave Radar and Radiometric Remote Sensing*. Ann Arbor, MI, USA: Univ. Michigan Press, 2015.
[34] M. W. Strudley, T. R. Green, and J. C. Ascough, "Tillage effects on soil hydraulic properties in space and time: State of the science," *Soil Tillage Res.*, vol. 99, no. 1, pp. 4–48, Apr. 2008.
[35] J. Alvarez-Mozos et al., "Influence of surface roughness spatial variability and temporal dynamics on the retrieval of soil moisture from SAR observations," *Sensors*, vol. 9, no. 1, pp. 463–489, Jan. 2009.
[36] P. Marzahn, D. Rieke-Zapp, and R. Ludwig, "Assessment of soil surface roughness statistics for microwave remote sensing applications using a simple photogrammetric acquisition system," *ISPRS J. Photogram. Remote Sens.*, vol. 72, pp. 80–89, Aug. 2012.

Zhuangzhuang Feng received the B.S. degree in surveying and mapping engineering from the Shandong University of Technology, Zibo, China, in 2019. He is currently working toward the Ph.D. degree in cartography and geographic information system with the Northeast Institute of Geography and Agroecology, Chinese Academy of Sciences, Changchun, China.

His research interests include passive/active microwave remote sensing of soil moisture, geophysical inversion model, and agricultural remote sensing.

Xingming Zheng (Member, IEEE) received the Ph.D. degree in cartography and geographic information system from the Northeast Institute of Geography and Agroecology, Chinese Academy of Sciences, Changchun, China, in 2012.

Since July 2012, he has been a Research Associate with the Northeast Institute of Geography and Agroecology, Chinese Academy of Sciences. His research interests include passive microwave remote sensing of soil moisture, geophysical inversion model, microwave radiative/scattering transfer model, and its application on crop canopy.

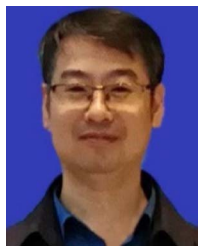

Xiaofeng Li (Member, IEEE) received the B.Sc. and M.Sc. degrees in mathematics from the Jilin University, Changchun, China, in 2002 and 2005, respectively, and the Ph.D. degree in remote sensing and geosciences from the Chinese Academy of Sciences, Changchun, China, in 2008.

He is currently a Professor with the Research Center of Remote Sensing and Geoscience, Northeast Institute of Geography and Agroecology, Chinese Academy of Sciences.

He has authored or coauthored more than 50 papers in journals and conference proceedings. His current research interests include the snow parameters inversion by remote sensing data, image processing, and agriculture remote sensing.

Dr. Li is the Chair of the IEEE GRSS Changchun chapter.

Huanjun Liu received the B.S. degree in land resources management from the Northeast Agricultural University, Harbin, China, in 2003, and the Ph.D. degree in cartography and geographic information system from the Northeast Institute of Geography and Agroecology, Chinese Academy of Sciences, Changchun, China, in 2008.

He is currently a Professor with the Northeast Institute of Geography and Agroecology, Chinese Academy of Sciences. His research interests include remote sensing, black soil conservation, and intelligent agriculture.

Zui Tao was born in China in 1984. He received the B.S. degree in cartography and geographic information system from the Henan University, Kaifeng, China, in 2005, the M.S. degree in cartography and geographic information system from the Wuhan University, Wuhan, China, in 2008, and the Ph.D. degree in cartography and geographic information system from the Institute of Remote Sensing and Digital Earth, Chinese Academy of Sciences (CAS), Beijing, China, in 2012.

He is currently a Research Assistant with the Aerospace Information Research Institute, CAS. His research interests include validation of remote sensing product, ecological, and environmental remote sensing.

Chunmei Wang received the Ph.D. degree in agricultural resources and environment from the China Agricultural University, Beijing, China.

She is currently an Associate Researcher with the Aerospace Information Research Institute, Chinese Academy of Sciences, Beijing, China. She has presided over more than 10 national Natural Science Foundation projects, National Science and Technology Support projects and industry topics, authorized to apply for 15 invention patents, authored/coauthored more than 60 academic papers (SCI 30). Her research interest include agricultural remote sensing and validation of remote sensing products.

Dr. Wang was the recipient of ten National and Ministry (provincial) level Science and Technology award.

Linghua Meng received the M.S. degree in land resources management from the Northeast Agricultural University, Harbin, China, in 2018, and the Ph.D. degree in cartography and geographic information system from the Northeast Institute of Geography and Agroecology, Chinese Academy of Sciences, Changchun, China, in 2023.

She is currently an Assistant Professor with the Northeast Institute of Geography and Agroecology, Chinese Academy of Sciences. Her research interests include remote sensing, black soil conservation, and intelligent agriculture.

Tianhao Guo received the B.S. degree in remote sensing science and technology from the Shandong University of Science and Technology, Qingdao, China, in 2021. He is currently working toward the M.S. degree in cartography and geographic information system with the Northeast Institute of Geography and Agroecology, Chinese Academy of Sciences, Changchun, China.

His research interests include algorithm development for the Google Earth Engine cloud platform, soil moisture inversion, and agricultural remote sensing applications.

Jia Zheng received the B.S. degree in cartography information science from the Harbin Normal University, Harbin, China, in 2022. She is currently working toward the M.S. degree in cartography and geographic information system with the Northeast Institute of Geography and Agroecology, Chinese Academy of Sciences, Changchun, China.

Her research interests include applications of agricultural remote sensing, including the monitoring of agricultural production processes and the analysis of the scale and distribution of agricultural plots.

Jinfeng Song received the B.S. degree in geographic information science from the Shaanxi Normal University, Xi'an, China, in 2023. She is currently working toward the M.S. degree in cartography and geographic information system with the Northeast Institute of Geography and Agroecology, Chinese Academy of Sciences, Changchun, China.

Her research interests include the construction of meteorological datasets and the application of remote sensing in agriculture.